Systematics of the α decay to vibrational 2^+ states

S. Peltonen,[1] D. S. Delion,[2] and J. Suhonen[1]
[1]*Department of Physics, University of Jyväskylä, POB 35, FIN-40351, Jyväskylä, Finland*
[2]*National Institute of Physics and Nuclear Engineering, Bucharest-Măgurele, POB MG-6, Romania*
(Received 14 January 2004; revised manuscript received 3 June 2004; published 27 April 2005)

We give a systematic analysis of α decays to low-lying 2^+ states in even-even nuclei. Collective excitations are considered within the spherical quasiparticle random-phase approximation. We use realistic G-matrix elements of the Bonn interaction as a residual two-body force. The only free parameters are the ratio between the isovector and isoscalar strengths and proton-neutron asymmetry. The formalism can reproduce the main experimental trends versus the excitation energy for both the $B(E2)$ values and the α-decay hindrance factors. We reproduced most of the available data by using one common parametrization. It turns out that the fine structure of the α decay is more sensitive than electromagnetic transitions as a tool for investigating nuclear interaction. With the adopted parametrization, we predict $B(E2)$ values and α-decay hindrance factors in even-even nuclei.

DOI: 10.1103/PhysRevC.71.044315 PACS number(s): 21.60.Jz, 23.60.+e, 27.70.+q, 27.80.+w

I. INTRODUCTION

The importance of the interplay between the Coulomb barrier and Q value on α decay was one of the most important discoveries in the early days of nuclear physics [1]. It explained the exponential dependence of half-lives upon the energy of the emitted particle (Q value). The proposed physical picture was very simple though it contradicted the classical intuition, namely, a preformed α particle inside the nucleus penetrates quantum mechanically the surrounding Coulomb barrier.

Later on, the preformation probability of the α cluster inside the nucleus was introduced within the R-matrix theory [2]. This approach takes into account nuclear structure details, because the cluster is built from two protons and two neutrons moving in some mean field and interacting with each other via two-body residual forces [3]. The so-called preformation amplitude is defined as the overlap of the initial wave function and the product between the daughter and α-particle wave functions. For transitions between ground states, it is a coherent superposition of many single-particle configurations, including states in continuum. Therefore, the decay width is not very sensitive to the nuclear mean field parameters. A systematic analysis of decay widths in even- and odd-mass actinide nuclei was performed in Ref. [4] by using the pairing approach for preformation amplitudes and spherical penetration factors. The most recent calculation, including super-heavy nuclei, within a similar model was performed in Ref. [5].

The situation changes for transitions to excited states. It turns out that the decay width is very sensitive to the structure of the wave function in the daughter nucleus. The fine structure in spectra of emitted α particles cannot be explained by only different Q values, due to the excitation energy of the daughter nucleus. It is known for a long time that the experimental hindrance factors (HF), extracting the exponential dependence upon the Coulomb barrier, are not constant [6]. The first calculations of α decay in rotational nuclei by using the coupled channels method were performed in Ref. [7]. Reference [8] estimated HF's in rotational nuclei by using the Fröman approach [9] for the barrier penetration but a simple phenomenological ansatz for the preformation factor. The first attempts to calculate HF's in vibrational nuclei within the quasiparticle random-phase approximation (QRPA) were performed in Refs. [10–12]. Later, Ref. [13] gave an explanation for the connection between the HF of the first excited 0^+ state and the neutron number for Pb isotopes. The calculation was performed in terms of proton-neutron pairing vibrations within the spherical RPA formalism using two major shells above the Fermi surface.

Only relatively recent experimental papers suggested that the α-decay fine structure could be a powerful tool for investigating nuclear structure details. In the last decade, this new kind of α-decay spectroscopy was mainly used to investigate 0^+ and 2^+ excited states in the Pb region by the ISOLDE collaboration [14–20] and more recently by the Liverpool-Jyväskylä-Helsinki collaboration [21]. There is also an increasing interest in α-decay experiments searching for fine structure in the U region [22]. Moreover, in the related field of proton emission, two papers [23,24] have shown that the influence of surface vibrations on the emission process is very important.

The aim of this article is to perform a systematic analysis of the α-decay fine structure for the lowest 2^+ states in even-even nuclei with moderate quadrupole deformations. Moreover, it will be clearly shown that the α-decay fine structure is a more sensitive probe of the 2^+-state wave function than is the electromagnetic transition deexiting this state. We use the formalism developed in our previous works [25,26]. In Sec. II, we give the necessary theoretical details. In Sec. III, we investigate the HF together with electromagnetic transitions for vibrational and transitional even-even nuclei. Here some theoretical predictions are also given. Conclusions are drawn in the last section.

II. THEORETICAL BACKGROUND

The microscopic description of the α decay to vibrational states within the QRPA formalism was given in Ref. [26]. In this section, we summarize the main theoretical details necessary to compute the decay width.

Let us consider an α-decay process

$$B \rightarrow A(k) + \alpha, \tag{2.1}$$

where $k = 0$ denotes the ground state (g.s.) and $k > 0$ some excited state in the daughter nucleus. We will describe low-lying collective states in terms of particle-hole excitations within the spherical QRPA. Indeed, Ref. [27] showed that the influence of the deformation on α decay is mainly given by the penetration through the Coulomb barrier.

The excited states are described by a phonon operator acting on the daughter ground state, taken as a core

$$|A(k)\rangle = \Gamma^{\dagger}_{\lambda\mu}(k)|A\rangle. \tag{2.2}$$

The QRPA phonon is defined, as usual, by

$$\Gamma^{\dagger}_{\lambda\mu}(k) = \sum_{\tau} \sum_{j_1 \leqslant j_2} \Big[X^{(k)}_{\lambda}(\tau j_1 j_2) A^{\dagger}_{\lambda\mu}(\tau j_1 j_2) - Y^{(k)}_{\lambda}(\tau j_1 j_2) A_{\lambda-\mu}(\tau j_1 j_2)(-)^{\lambda-\mu} \Big], \tag{2.3}$$

where $A^{\dagger}_{\lambda\mu}(\tau j_1 j_2)$ denotes the quasiparticle creation operator of the pair $(\tau j_1 j_2)$, with $\tau = \pi$ for protons and $\tau = \nu$ for neutrons. Here j is a short-hand notation for spherical quantum numbers, i.e., single-particle energy ϵ, angular momentum l, and total spin j. We will consider quadrupole phonon operators with $\lambda = 2$ to describe low-lying 2^+ collective excitations.

The amplitude of the decay process (2.1), called α-particle preformation amplitude, is given as an overlap integral over the internal coordinates of the daughter nucleus and the emitted cluster [3], i.e.,

$$\begin{aligned} F^{(k)}_{\lambda\mu}(\mathbf{R}) &\equiv \langle A|(-)^{\lambda-\mu}\Gamma_{\lambda-\mu}(k)\Psi_{\alpha}|B\rangle \\ &= \int d\xi_A d\xi_{\alpha} \big[\Psi^{(k)}_{A}(\xi_A)\big]^{*} \Psi^{*}_{\alpha}(\xi_{\alpha})\Psi_{B}(\xi_B), \end{aligned} \tag{2.4}$$

where ξ denotes the internal coordinates and $\mathbf{R}$ the center-of-mass coordinate of the α-daughter system. The preformation amplitude squared is the probability of having an α-decaying configuration inside the initial state. The above integral depends only upon the relative radius between the daughter nucleus and the emitted cluster.

We neglect the core-cluster antisymmetrization, because we estimate the overlap for distances beyond the geometrical nuclear radius, where the Pauli principle becomes less important [28]. For $k = 0$, one uses the ground state in the daughter nucleus instead of a QRPA excitation.

The most important ingredient of our calculation is the single-particle mean field, generating proton and neutron eigenstates. The single-particle wave functions are given in the harmonic oscillator (ho) representation as follows

$$\begin{aligned} \psi_{\tau\epsilon ljm}(\mathbf{r}, s) &\equiv \langle \mathbf{r}, s|a^{\dagger}_{\tau\epsilon ljm}|0\rangle \\ &= \sum_{n} c_n(\tau\epsilon lj)\mathcal{R}_{nl}(\beta r^2)\big[i^l Y_l(\hat{r}) \otimes \chi_{\frac{1}{2}}(s)\big]_{jm}. \end{aligned} \tag{2.5}$$

Here $a^{\dagger}_{\tau\epsilon ljm}$ denotes the single-particle creation operator. The expansion coefficients $c_n(\tau\epsilon lj)$ are provided by the diagonalization procedure in the spherical ho basis $\mathcal{R}_{nl}(\beta r^2)$. They depend upon the standard ho parameter, defined as

$$\beta = f\frac{M_N\omega}{\hbar}, \tag{2.6}$$

where M_N is the nucleonic mass and $\hbar\omega = 41A^{-1/3}$. As shown in Refs. [5,29] the spectroscopic properties, connected with the bound spectrum, practically do not depend upon the value of the size parameter f. Moreover, Ref. [30] pointed out that the error in expanding the radial wave function in terms of the harmonic oscillator basis remains practically a constant in the interval $f \in [0.5, 1.2]$.

The radial part of the preformation amplitude for transitions to excited states is given by the following superposition

$$F^{(k)}_{\lambda}(R) = \sum_{N_{\alpha}} W^{(k)}(N_{\alpha}\lambda)\mathcal{R}_{N_{\alpha}\lambda}(4\beta R^2), \tag{2.7}$$

where the $W^{(k)}$ coefficient is given in App. A of Ref. [26]. The preformation amplitude, connecting the ground states of the two nuclei, is obtained in a similar way with $k = 0$, where the $W^{(0)}$ coefficient is defined in the same appendix. We stress the fact that the radial ho wave function $\mathcal{R}_{NL}(4\beta R^2)$ depends on four times the single-particle parameter β, due to the Talmi-Moshinsky transformation from absolute to relative and center-of-mass coordinates.

The most important ingredients entering the W coefficients in the above relations and expressing the nuclear structure details are the expansion coefficients of the mother in terms of the daughter wave function. For transitions to excited states, they are given by

$$\begin{aligned} |B\rangle = \frac{1}{2}\Bigg\{ &\sum_{j_1=j_2}\sum_{j_3\leqslant j_4} B(\pi j_1 j_2; \nu j_3 j_4)(a^{\dagger}_{\pi j_1} \otimes a^{\dagger}_{\pi j_2})_0\hat{\lambda} \\ &\times [(a^{\dagger}_{\nu j_3} \otimes a^{\dagger}_{\nu j_4})_{\lambda} \otimes \Gamma^{\dagger}_{\lambda}(k)]_0|A\rangle \\ &+ \sum_{j_1=j_2}\sum_{j_3\leqslant j_4} B(\nu j_1 j_2; \pi j_3 j_4)(a^{\dagger}_{\nu j_1} \otimes a^{\dagger}_{\nu j_2})_0\hat{\lambda} \\ &\times [(a^{\dagger}_{\pi j_3} \otimes a^{\dagger}_{\pi j_4})_{\lambda} \otimes \Gamma^{\dagger}_{\lambda}(k)]_0|A\rangle \Bigg\}, \end{aligned} \tag{2.8}$$

where $\hat{\lambda} = \sqrt{2\lambda + 1}$. By expressing the particle operators in terms of quasiparticle operators, one obtains the following results

$$\begin{aligned} B(\pi j_1 j_2; \nu j_3 j_4) &= B^{(0)}(\pi j_1 j_2)B^{(k)}(\nu j_3 j_4), \\ B(\nu j_1 j_2; \pi j_3 j_4) &= B^{(0)}(\nu j_1 j_2)B^{(k)}(\pi j_3 j_4), \end{aligned} \tag{2.9}$$

where the two terms are given, respectively, by

$$\begin{aligned} B^{(0)}(\tau j_1 j_2) &= \delta_{j_1 j_2}\frac{\hat{j}_1}{2}u_{\tau j_1}v_{\tau j_1}, \\ B^{(k)}(\tau j_3 j_4) &= \frac{1}{\sqrt{1+\delta_{j_3 j_4}}}\big[u_{\tau j_3}u_{\tau j_4}Y^{(k)}_{\lambda}(\tau j_3 j_4) \\ &\quad - v_{\tau j_3}v_{\tau j_4}X^{(k)}_{\lambda}(\tau j_3 j_4)\big]. \end{aligned} \tag{2.10}$$

Here u, v denote BCS and X, Y QRPA amplitudes. In particular, for a g.s. to g.s. transition, one obtains the expansion given in Ref. [27].

The decay width is derived from the continuity equation and it is proportional to the asymptotic value of the radial wave function amplitude squared. The matching condition between the preformation amplitude and the outgoing Coulomb wave, for some radius R inside the Coulomb potential, gives the expression

$$\Gamma_\lambda^{(k)} = \hbar v \lim_{r\to\infty} \left|g_\lambda^{(k)}(r)\right|^2 = \left\{\frac{2\kappa R}{[G_\lambda(\kappa R)]^2}\right\}\left\{\frac{R\hbar^2}{2\mu}\left[F_\lambda^{(k)}(R)\right]^2\right\} \equiv \mathcal{P}_\lambda(E, R)\mathcal{F}_\lambda^{(k)}(R), \tag{2.11}$$

where v is the center-of-mass velocity, κ the momentum of the emitted α particle and R the center-of-mass radius. Note that the meaning of the letter Γ is different from the definition of the QRPA phonon (2.3). This quantity is a product of two functions, the penetrability $\mathcal{P}_\lambda$ and preformation probability $\mathcal{F}_\lambda$ (the so-called reduced width squared), which strongly depend upon the radius R. However, the final result $\Gamma_\lambda^{(k)}$ should be a constant in a region of several fm around the geometrical touching point. This is an important accuracy test for our calculations, and it was analyzed in detail in Ref. [26].

The HF of the first collective 2^+ state we estimate as the ratio between the corresponding "strengths" of the preformation factors, i.e.,

$$\mathrm{HF} = \frac{\left\langle R\left[F_0^{(0)}(R)\right]^2\right\rangle}{\left\langle R\left[F_2^{(1)}(R)\right]^2\right\rangle}, \tag{2.12}$$

where by brackets we denote the mean values, considered over the interval $R \geqslant R_c$, beyond the touching radius

$$R_c = 1.2\left(A_\alpha^{1/3} + A_A^{1/3}\right), \tag{2.13}$$

including the last two maxima of preformation amplitudes. We showed in Ref. [26] that the ratio of averaged quantities in (2.12) practically does not depend upon the matching radius. This definition is consistent with the experimental estimate given by

$$\mathrm{HF}_{\mathrm{exp}} = \frac{\Gamma_{\mathrm{exp}}^{(0)}}{\Gamma_{\mathrm{exp}}^{(1)}}\frac{\mathcal{P}_2(E - E_{2^+}, R)}{\mathcal{P}_0(E, R)}, \tag{2.14}$$

where $\Gamma^{(k)}$, with $k = 0$, denotes the decay width corresponding to a transition between ground states, and $k = 1$ denotes the width associated with decay transition to the first 2^+ eigenstate. According to Rasmussen [6], the hindrance factor contains the pentration through a barrier with a sharp internal potential. As we will show later, the comparison between the two estimates gives a difference of less than a factor of 2, i.e., within the experimental error. Anyway, we prefer the estimate given by (2.14) because it depends only upon the well-defined irregular function $G_l(\kappa R)$, generated by the external Coulomb repulsion, and does not contain any arbitary internal potential.

The effect of the deformation, given by the Fröman matrix [9] for the penetration part, was recently investigated in Ref. [5], where it was shown that for $|\beta_2| \leqslant 0.2$ the effect of the barrier deformation is less than a factor of 2. Thus, the use of a deformed penetration for both transitions will give similar corrections and will not affect their ratio. This approach was used in Ref. [8] to investigate transitions to rotational states.

We also computed another useful quantity, namely, the spectroscopic factor, defined as

$$S_\alpha^{(k)} = \int_0^\infty \left|RF_\lambda^{(k)}(R)\right|^2 dR. \tag{2.15}$$

It gives the order of magnitude of the α-particle probability inside the nucleus.

Concerning the electromagnetic quadrupole transition, we used the standard relation for the reduced matrix element, namely,

$$\langle 0||T_2||k\rangle = \sum_\tau \sum_{j_1 \leqslant j_2} \xi_{\tau j_1 j_2}\left[X_\lambda^{(k)}(\tau j_1 j_2) + Y_\lambda^{(k)}(\tau j_1 j_2)\right],$$
$$\xi_{\tau j_1 j_2} = \frac{e_\tau}{\sqrt{1+\delta_{j_1 j_2}}}\langle \tau j_1||r^2 Y_2||\tau j_2\rangle\left(u_{\tau j_1} v_{\tau j_2} + v_{\tau j_1} u_{\tau j_2}\right), \tag{2.16}$$

where e_τ denotes the effective charge and Y_2 the quadrupole spherical function.

III. $B(E2)$ AND HF SYSTEMATICS ALONG ISOTOPE CHAINS

A. Analysis of the experimental data

We will analyze α decays to low-lying 2^+ states in even-even nuclei with moderate quadrupole deformations, $|\beta_2| \leqslant 0.2$, i.e., in the so-called vibrational and transitional nuclei. At the same time, we will connect this strong interacting process with electromagnetic transitions in the daughter nucleus.

Concerning $B(E2)$ values, there are many available data, e.g., those in Ref. [31]. In Fig. 1 we plotted them as a function of the excitation energy for those even-even nuclei where

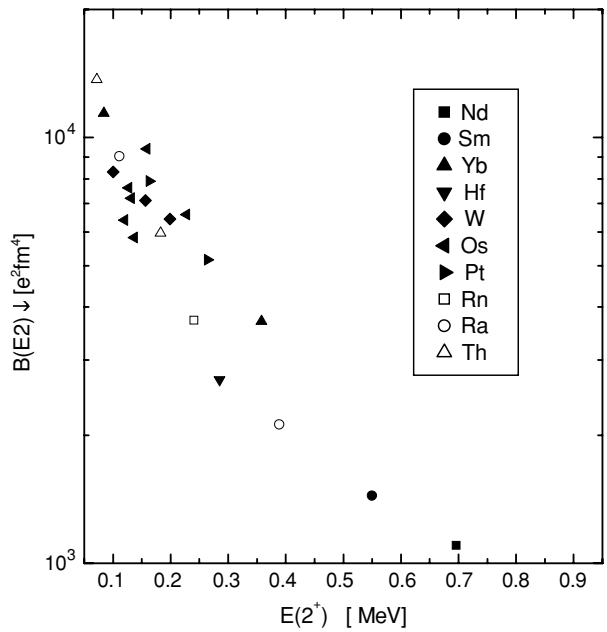

FIG. 1. Experimental $B(E2)$ values versus E_{2^+}.

TABLE I. Experimental hindrance factors [33] according to Rasmussen [6] and Eq. (2.14) (last two columns). The first columns give the three regions and the states in the abscissa of Fig. 2. The next columns give the charge and atomic numbers, energy of the 2^+ state [33], and quadrupole deformation [34]. Experimental errors for excitation energies and HF's are also given.

Region	i	Z	N	A	E_{2^+} (keV)	β_2	$HF_{\rm exp}^{\rm (Ras)}$	$HF_{\rm exp}$
(A)	1	76	96	172	228.0 ± 0.2	0.190	38 ± 19	21.287
	2	76	98	174	158.7 ± 0.3	0.226	3.3 ± 1.6	1.828
	3	78	98	176	263 ± 1	0.171	$152 \pm ??$	85.688
	4	78	100	178	170.7 ± 0.7	0.254	$31.3 \pm ??$	14.043
	5	78	102	180	$153 \pm ??$	0.265	47 ± 10	26.571
(B)	6	84	110	194	319 ± 10	0.026	110 ± 40	66.379
	7	84	112	196	463 ± 1	0.136	180 ± 60	173.541
	8	84	120	204	684.342 ± 0.010	0.009	1.25 ± 0.11	0.706
	9	84	122	206	703 ± 3	−0.018	6.9 ± 0.4	3.947
	10	84	124	208	686.528 ± 0.020	−0.018	1.43 ± 0.15	0.830
(C)	11	84	130	214	609.31 ± 0.06	−0.008	4.8 ± 0.8	2.774
	12	84	132	216	549.73 ± 0.05	0.020	3.2 ± 0.5	1.775
	13	84	134	218	511 ± 2	0.039	$1.9 \pm ??$	1.052
	14	86	130	216	461.9 ± 0.2	0.008	2.6 ± 0.8	1.565
	15	86	132	218	324.22 ± 0.05	0.040	1.45 ± 0.04	0.852
	16	86	134	220	240.986 ± 0.006	0.111	1.08 ± 0.01	0.622
	17	86	136	222	186.211 ± 0.013	0.137	0.96 ± 0.01	0.546
	18	88	130	218	389.2 ± 0.2	0.020	2.0 ± 0.7	1.219
	19	88	132	220	178.37 ± 0.09	0.103	0.96 ± 0.07	0.572
	20	88	134	222	111.12 ± 0.02	0.130	1.08 ± 0.02	0.650
	21	88	136	224	84.373 ± 0.003	0.164	0.90 ± 0.03	0.536
	22	90	132	222	$183.3 \pm ??$	0.111	1.4 ± 0.5	0.830
	23	90	134	224	93 ± 4	0.164	1.00 ± 0.07	0.579

α-decay half-lives to the ground state are measured. One can observe a universal systematic decreasing behavior versus the excitation energy, almost independent of the considered chain. This quantity is not very sensitive to other nuclear structure details, because of the collective character of the 2^+ state. Indeed, Ref. [32], showed that one has the following empirical relation between the $B(E2)$ value and E_{2^+} energy

$$B(E2) = \frac{cZ^2}{A^{2/3}E_{2^+}}, \tag{3.1}$$

where Z is the charge and A the mass number of the nucleus.

The situation is quite different concerning the α decay. At present, the amount of available HF data is limited; see, e.g. Ref. [33]. They are given in Table I. The last two columns given the experimental HF's, estimated according to the Rasmussen procedure $\mathrm{HF}_{\rm exp}^{\rm (Ras)}$ [6] and by using Eq. (2.14) $\mathrm{HF}_{\rm exp}$, respectively. One can see that they differ by a factor less than 2. Anyway, we prefer to use the simple definition (2.14), which is free of any potential parameter. We plotted the logarithm of the $\mathrm{HF}_{\rm exp}$ in Fig. 2 by a solid line, connecting experimental points along a given neutron chain. In the same figure, experimental values of the 2^+ energy are given by dashes. The labels on the abscissa correspond to the numbers in the first column of Table I. We divided the figure into three regions,

$$\begin{aligned} &\text{(A)}: Z < 82, \quad N < 126, \\ &\text{(B)}: Z > 82, \quad N < 126, \\ &\text{(C)}: Z > 82, \quad N > 126. \end{aligned} \tag{3.2}$$

First of all, one notices an opposite tendency compared to $B(E2)$ data, namely, a general decreasing trend by decreasing the excitation energy in the daughter nucleus. This is given by the solid lines along each isotope chain. It turns out that

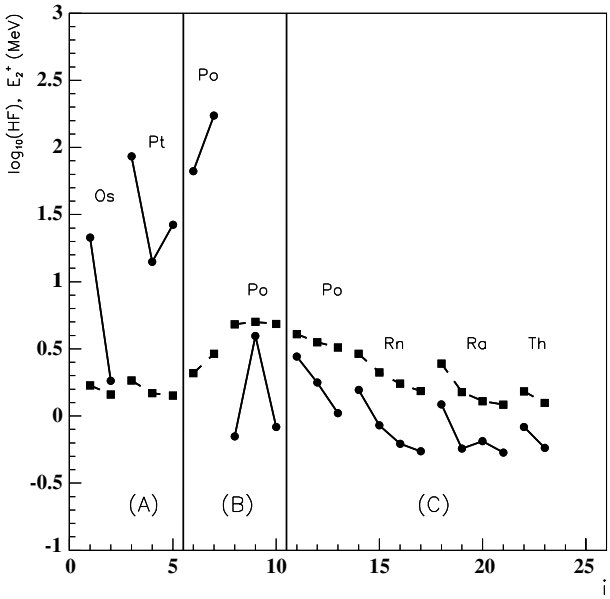

FIG. 2. Experimental hindrance factors (solid lines) and E_{2^+} (dashed lines) versus the state number in Table I.

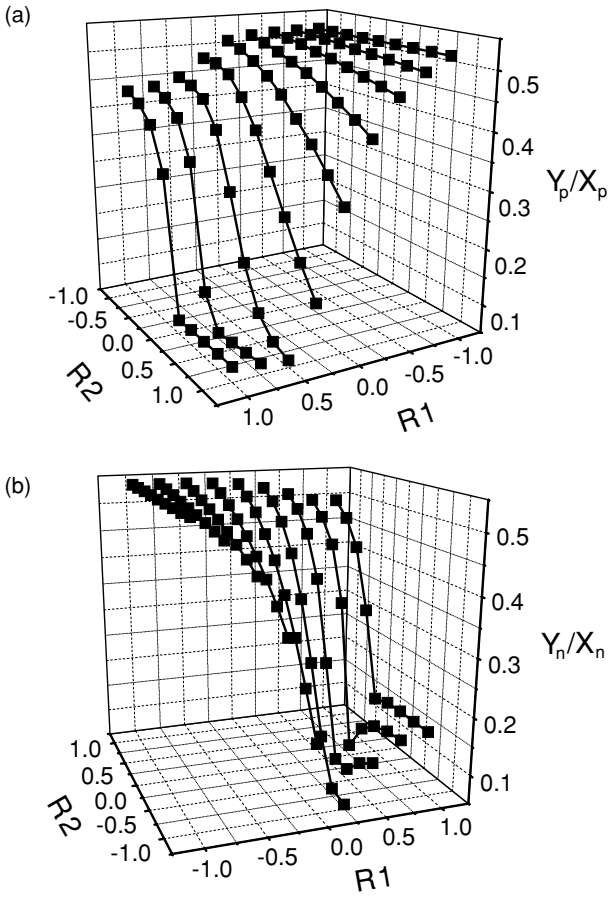

FIG. 3. The proton and neutron ratio of summed QRPA amplitudes squared Y_τ^2/X_τ^2, where (a) $\tau = \pi$ and (b) $\tau = \nu$, versus the ratios R_1 and R_2. The decay process is ^{220}Ra $\rightarrow$ ^{216}Rn.

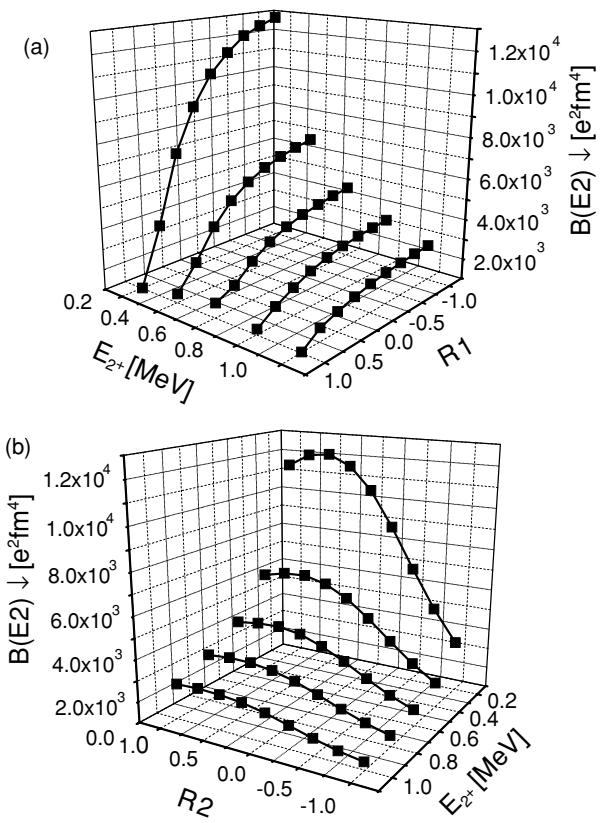

FIG. 4. $B(E2)$ values as a function of (a) E_{2^+}, R_1 for $R_2 = 0$ and (b) E_{2^+}, R_2 for $R_1 = 0$. The decay process is ^{220}Ra $\rightarrow$ ^{216}Rn.

the HF's in all the regions, apart from nuclei close to magic numbers, satisfy the following empirical rule

$$\log_{10}(\mathrm{HF}) = aE_{2^+} + b, \tag{3.3}$$

with a common coefficient for each of the regions. As a general rule, the slope of this dependence for region (A) is larger than for (C), i.e., $a_{(\mathrm{A})} > a_{(\mathrm{C})}$. The situation in region (B), describing Po isotopes as daughter nuclei, is more complex. Here one has a phase transition along Po isotopes, from large HF's, for neutron-deficient isotopes, to small ones. Unfortunately the available experimental values do not describe the full chain of Po isotopes. It seems that the left side of the region (B) has a behavior similar to that of (A), while the right one resembles the behavior of region (C).

This behavior is less universal than the trend of electromagnetic transitions. Thus, according to the available experimental material, one concludes that the α-decay fine structure is more sensitive to concrete nuclear structure details than the corresponding electromagnetic transition. This makes the study of the α decay to excited states a useful tool for investigating the properties of collective states.

B. Analysis of the QRPA features

In our analysis we will try to explain the above discussed experimental features within our QRPA formalism for collective 2^+ excitations. We used the universal parametrization of the Woods-Saxon potential, which is suitable for generating proton and neutron single-particle spectra, especially for nuclei around Pb region [35]. In the Woods-Saxon diagonalization procedure, we considered $N = 18$ major shells. In our calculation, we considered only 20 proton and 18–19 neutron *sp* states around the corresponding Fermi surfaces. Therefore, to simplify the calculations, we considered a smaller number of configurations than the value necessary to reproduce the absolute width [5]. Our analysis showed that indeed the ratio of decay widths for transitions to excited and ground state, i.e. HF, is sensitive only to spherical single-particle orbitals around the Fermi level. Moreover, HF is insensitive to the size used for parameter f because both preformation factors are changed in the same way. We used a standard value for this parameter, namely $f = 1$.

In Ref. [26] we used a modified surface δ residual interaction by decoupling strength parameters for different multipolarities. In our present analysis, we use realistic G-matrix elements generated by starting from the Bonn one-boson-exhange potential [36]. The quasiparticles are generated by the monopole part of the two-body interaction. The pairing strengths have been adjusted separately for protons and neutrons to reproduce experimental gap values. We considered

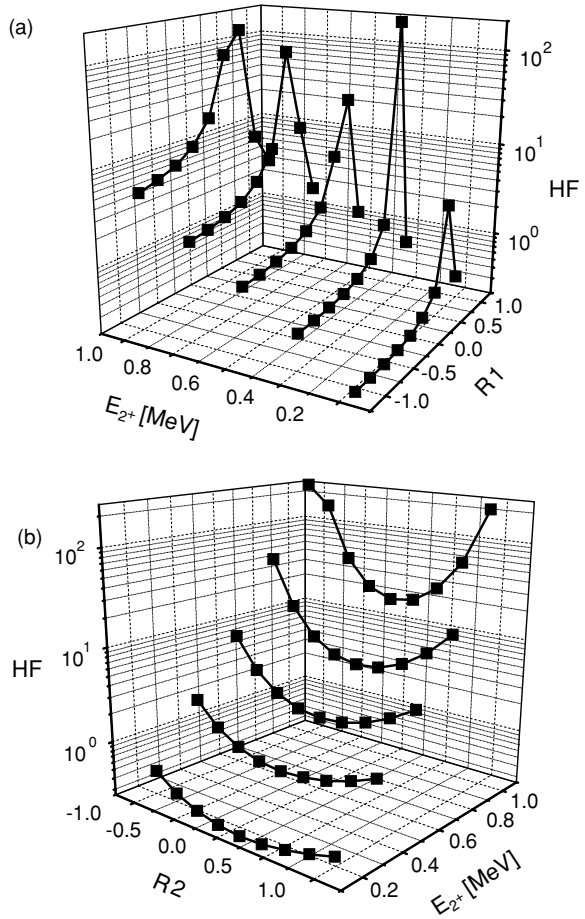

FIG. 5. Hindrance factor as a function of (a) E_{2^+}, R_1 for $R_2 = 0$ and (b) E_{2^+}, R_2 for $R_1 = 0$. The decay process is $^{220}\mathrm{Ra} \rightarrow {}^{216}\mathrm{Rn}$.

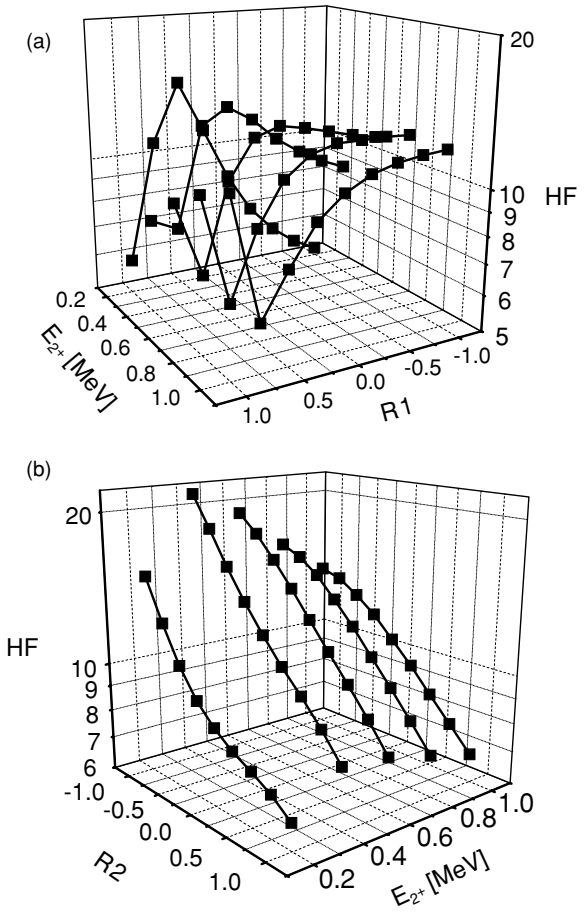

FIG. 6. Same as Fig. 5, but for the decay process $^{180}\mathrm{Hg} \rightarrow {}^{176}\mathrm{Pt}$.

in our calculations only superfluid nuclei, i.e., for both mother and daughter nuclei, Z and N are not magic numbers.

To investigate the quadrupole-quadrupole part we used three parameters, namely the proton-proton V_π, neutron-neutron V_ν, and proton-neutron strengths $V_{\pi\nu}$. This allows us to schematically rewrite the residual interaction in the form

$$\begin{aligned} &-V_\pi Q_\pi Q_\pi^\dagger - V_\nu Q_\nu Q_\nu^\dagger - V_{\pi\nu}\left[Q_\pi Q_\nu^\dagger + Q_\nu Q_\pi^\dagger\right] \\ &\quad = -V_+ Q_+ Q_+^\dagger - V_- Q_- Q_-^\dagger - V_\pm\left[Q_+ Q_-^\dagger + Q_- Q_+^\dagger\right], \end{aligned} \tag{3.4}$$

in terms of isoscalar Q_+ and isovector quadrupole components Q_-, defined as

$$Q_+ = Q_\pi + Q_\nu, \quad Q_- = Q_\pi - Q_\nu. \tag{3.5}$$

The corresponding strengths can be written as

$$\begin{aligned} V_+ &= \frac{V_\pi + V_\nu + 2V_{\pi\nu}}{4}, \\ V_- &= \frac{V_\pi + V_\nu - 2V_{\pi\nu}}{4}, \\ V_\pm &= \frac{V_\pi - V_\nu}{4}. \end{aligned} \tag{3.6}$$

Our analysis depends on only two parameters, namely, the following ratios

$$\begin{aligned} R_1 &\equiv V_-/V_+ = \frac{V_\pi + V_\nu - 2V_{\pi\nu}}{V_\pi + V_\nu + 2V_{\pi\nu}}, \\ R_2 &\equiv \frac{2V_\pm}{V_+ + V_-} = \frac{V_\pi - V_\nu}{V_\pi + V_\nu}, \end{aligned} \tag{3.7}$$

because, after fixing them, we adjust V_+ to obtain the experimental value of the energy E_{2^+}. In what follows, we call ratio R_2 the proton-neutron asymmetry.

The QRPA amplitudes X, Y in Eq. (2.3) contain the information about the nuclear structure in the HF and $B(E2)$ values. These are the key ingredients connecting the two kinds of transition. Thus, we will characterize the "collectivity" of the first excited state, with $k = 1$, by the following proton and neutron ratios

$$Y_\tau^2 \Big/ X_\tau^2 \equiv \sum_{j_1 \leqslant j_2} Y_{\tau j_1 j_2}^2(1) \Bigg/ \sum_{j_1 \leqslant j_2} X_{\tau j_1 j_2}^2(1), \quad \tau = \pi, \nu. \tag{3.8}$$

The behavior of these ratios is strongly dependent upon the values of R_1 and R_2. This is shown in Fig. 3 for protons/neutrons for the decay process $^{220}\mathrm{Ra} \rightarrow {}^{216}\mathrm{Rn}$.

TABLE II. Experimental and predicted HF's (in the last two columns) for α emitters below Pb. First four columns give the charge, mass number, quadrupole deformation [34] and E_{2^+} [31] in the daughter nucleus. The sixth and seventh columns give experimental $B(E2)$ values [31] and theoretical predictions. The interaction parameters are $R_1 = 0$, $R_2 = -0.75$. The fifth column gives the corresponding values of the strength V_+, according to Eqs. (3.6) and (3.7).

Z	A	β_2	E_{2^+}	V_+	$B(E2)_{\rm exp}$	$B(E2)$	$\rm HF_{exp}$	HF
60	144	0.149	0.696	0.722	$1.10\ 10^3$	$5.16\ 10^2$	–	$1.32\ 10^0$
62	146	0.155	0.747	0.709	–	$4.66\ 10^2$	–	$2.64\ 10^0$
62	148	0.161	0.550	0.671	$1.44\ 10^3$	$9.69\ 10^2$	–	$1.11\ 10^0$
64	148	0.156	0.784	0.716	–	$5.94\ 10^2$	–	$1.73\ 10^0$
64	150	0.161	0.638	0.657	–	$8.13\ 10^2$	–	$2.00\ 10^0$
66	150	0.153	0.804	0.706	–	$6.40\ 10^2$	–	$1.48\ 10^0$
68	152	−0.018	0.808	0.724	–	$8.31\ 10^2$	–	$1.22\ 10^0$
68	154	0.143	0.561	0.675	–	$1.58\ 10^3$	–	$6.35\ 10^{-1}$
70	154	−0.008	0.821	0.702	–	$5.85\ 10^2$	–	$2.47\ 10^0$
70	156	0.125	0.536	0.669	–	$1.65\ 10^3$	–	$6.85\ 10^{-1}$
70	158	0.161	0.358	0.618	$3.70\ 10^3$	$2.31\ 10^3$	–	$5.25\ 10^{-1}$
72	156	0.035	0.858	0.606	–	$3.08\ 10^2$	–	$3.97\ 10^1$
72	158	0.107	0.476	0.600	–	$1.02\ 10^3$	–	$2.89\ 10^0$
72	160	0.152	0.390	0.624	–	$2.40\ 10^3$	–	$1.18\ 10^0$
72	162	0.180	0.285	0.570	$2.70\ 10^3$	$3.54\ 10^3$	–	$1.08\ 10^0$
74	162	0.134	0.450	0.542	–	$1.09\ 10^3$	–	$3.67\ 10^1$
74	164	0.161	0.332	0.564	–	$2.48\ 10^3$	–	$5.89\ 10^0$
74	166	0.181	0.252	0.532	–	$3.24\ 10^3$	–	$2.49\ 10^0$
76	166	0.134	0.431	0.511	–	$1.01\ 10^3$	–	$3.77\ 10^1$
76	168	0.162	0.341	0.477	–	$1.48\ 10^3$	–	$7.20\ 10^1$
76	170	0.171	0.287	0.487	–	$1.67\ 10^3$	–	$1.57\ 10^1$
76	172	0.190	0.228	0.490	$6.60\ 10^3$	$2.62\ 10^3$	$2.13\ 10^1$	$2.85\ 10^1$
78	172	0.126	0.457	0.472	–	$9.80\ 10^2$	–	$1.07\ 10^1$
78	174	0.153	0.394	0.499	–	$1.02\ 10^3$	–	$1.31\ 10^1$
78	176	0.171	0.264	0.514	$5.16\ 10^3$	$1.90\ 10^3$	$8.57\ 10^1$	$1.55\ 10^1$

We stress that $R_1 = 0, R_2 = 0$ corresponds to a pure isoscalar interaction with a common nucleon-nucleon interaction strength, i.e., $V_\pi = V_\nu = V_{\pi\nu}$. In Ref. [26] we investigated this case for transitions from the Rn isotopes. Now we have extended our analysis to the interval $-1 < R_1 < 1$. In particular, when $R_1 = -1$, $R_2 = 0$, one has $V_\pi = V_\nu = 0$ and only the effective interaction between proton and neutron systems $V_{\pi\nu}$ has a nonvanishing value. In the opposite extreme, i.e., for $R_1 = 1$, $R_2 = 0$, the effective interaction between proton and neutron systems vanishes, $V_{\pi\nu} = 0$. We also considered in our analysis a nonvanishing proton-neutron asymmetry parameter R_2, which was equal to zero in our previous reference.

First, we analyzed the behavior of the $B(E2)$ value as a function of the ratio R_1 and R_2 and excitation energy E_{2^+}. We used in Eq. (2.16) the bare charges $e_\pi = 1, e_\nu = 0$. As a typical example, in Fig. 4(a) we plot $B(E2)$ values as a function of R_1 and excitation energy for $R_2 = 0$ by considering the decay process $^{220}\rm Ra \rightarrow {}^{216}Rn$. In Fig. 4(b), we give a similar plot versus R_2 and excitation energy for $R_1 = 0$. One can see that the $B(E2)$ value decreases when R_1 and the excitation energy increase or when R_2 decreases. It is interesting that the dependence of the $B(E2)$ value on these variables is monotonic, except in the vicinity of $R_1 = 1$. This feature explains the universal behavior of experimental data, seen in Fig. 1. Therefore, we conclude that the QRPA is able to reproduce the experimental behavior of the $B(E2)$ value versus the excitation energy E_{2^+}.

Let us now consider the main quantity in our analysis, namely, the HF. In the three-dimensional Fig. 5(a), we plot this quantity as a function of the ratio R_1 (with $R_2 = 0$) and E_{2^+} for the decay process $^{220}\rm Ra \rightarrow {}^{216}Rn$ of region (C); while in Fig. 5(b), we plot the HF versus the ratio R_2 (with $R_1 = 0$) and E_{2^+}. One observes, first of all, that the HF has much stronger dependence upon R_1, R_2, and E_{2^+} than the $B(E2)$ value. This means that the HF is more sensitive to the Y_τ^2/X_τ^2 ratio than is the electromagnetic transition. On the other hand, as a general rule, the HF increases with the increase of the excitation energy, thus reproducing the main trend of experimental data in Fig. 2. In Fig. 6 we made the same plots as in Fig. 5 but for the transition $^{180}\rm Hg \rightarrow {}^{176}Pt$ from region (A). Comparing these two sets of figures one immediately notices a more complex behavior of the slopes of the HF vs E_{2^+} curves. Moreover, our numerical analysis for several decay processes showed that, as a general rule, the slope versus the excitation energy is larger in region (A) than in region (C). Thus, once again, the QRPA is able to reproduce the main experimental trends.

C. Systematic predictions

Finally, we computed the $B(E2)$ values and HF's for several vibrational and transitional nuclei, where α-decay half-lives were measured. We studied the dependence of the standard mean square deviation from experimental data both for the $B(E2)$ and HF's. It turned out that this quantity

TABLE III. Same as in Table II, but for α emitters above Pb. The interaction parameters are $R_1 = 0$, $R_2 = -0.75$, except for the first two nuclei, where $R_1 = 0.5$, $R_2 = -0.75$.

Z	A	β_2	E_{2^+}	V_+	$B(E2)_{\rm exp}$	$B(E2)$	$\rm HF_{exp}$	HF
84	194	0.026	0.319	0.544	–	$4.55\ 10^{+2}$	$6.64\ 10^{+1}$	$9.80\ 10^{+1}$
84	196	0.136	0.463	0.519	–	$4.21\ 10^{+2}$	$1.74\ 10^{+2}$	$1.25\ 10^{+2}$
84	200	0.009	0.666	0.530	–	$5.34\ 10^{+2}$	–	$1.94\ 10^{+2}$
84	202	0.009	0.677	0.529	–	$4.80\ 10^{+2}$	–	$1.85\ 10^{+1}$
84	204	0.009	0.684	0.503	–	$3.03\ 10^{+2}$	$7.06\ 10^{-1}$	$3.25\ 10^{+0}$
84	206	−0.018	0.700	0.521	–	$2.39\ 10^{+2}$	$3.95\ 10^{+0}$	$1.32\ 10^{+0}$
84	212	0.045	0.727	0.745	–	$3.25\ 10^{+2}$	–	$1.19\ 10^{+1}$
84	214	−0.008	0.609	0.720	–	$6.41\ 10^{+2}$	$2.77\ 10^{+0}$	$3.92\ 10^{+0}$
84	216	0.020	0.550	0.691	–	$8.89\ 10^{+2}$	$1.77\ 10^{+0}$	$4.04\ 10^{+0}$
84	218	0.039	0.511	0.594	–	$5.81\ 10^{+2}$	$1.05\ 10^{+0}$	$3.37\ 10^{+1}$
86	202	−0.104	0.504	0.529	–	$9.17\ 10^{+2}$	–	$7.36\ 10^{+2}$
86	204	−0.087	0.543	0.544	–	$8.96\ 10^{+2}$	–	$4.09\ 10^{+1}$
86	206	−0.044	0.575	0.537	–	$6.47\ 10^{+2}$	–	$5.20\ 10^{+0}$
86	208	−0.026	0.636	0.494	–	$2.90\ 10^{+2}$	–	$3.84\ 10^{+0}$
86	214	0.008	0.694	0.750	–	$6.79\ 10^{+2}$	–	$4.63\ 10^{+0}$
86	216	0.008	0.465	0.730	–	$1.61\ 10^{+3}$	$1.56\ 10^{+0}$	$1.60\ 10^{+0}$
86	218	0.040	0.324	0.695	–	$2.57\ 10^{+3}$	$8.52\ 10^{-1}$	$9.43\ 10^{-1}$
86	220	0.111	0.241	0.663	$3.72\ 10^{+3}$	$3.28\ 10^{+3}$	$6.22\ 10^{-1}$	$8.05\ 10^{-1}$
88	208	−0.104	0.520	0.545	–	$9.15\ 10^{+2}$	–	$2.12\ 10^{+1}$
88	210	−0.053	0.603	0.527	–	$4.85\ 10^{+2}$	–	$5.02\ 10^{+0}$
88	216	0.008	0.688	0.747	–	$9.81\ 10^{+2}$	–	$5.20\ 10^{+0}$
88	218	0.020	0.389	0.720	$2.12\ 10^{+3}$	$2.38\ 10^{+3}$	$1.22\ 10^{+0}$	$1.17\ 10^{+0}$
90	218	0.008	0.689	0.747	–	$1.49\ 10^{+3}$	–	$9.70\ 10^{+0}$
90	220	0.030	0.373	0.719	–	$4.29\ 10^{+3}$	–	$2.63\ 10^{+0}$

has a pronounced minimum concerning the $B(E2)$ value for $R_1 = 0$, $R_2 = -0.75$ in region (C) and the right side of region (B). In region (A), this quantity is not sensitive to R_1 for the interval $R_1 \in [-1, 0]$. Concerning the HF, we found that the minimal standard square deviation is achieved close to the same values $R_1 = 0$, $R_2 = -0.75$.

Therefore, we chose these values to make predictions for both the $B(E2)$ values and the HF's for the other nuclei. In the last column of Table II, we give the HF's, as predictions by our model, for measured α decays connecting ground states of even-even nuclei with moderate deformations in the region $Z < 82$. We considered only those nuclei with $E_{2^+} \geqslant 0.2$ MeV. Here, we also give the corresponding $B(E2)$ values. One can see that the electromagnetic transitions are rather well reproduced, together with most of the measured HF's. In Table III we give similar predictions for even-even α emitters with $Z > 82$. We divided the table into the abovementioned (B) (upper part) and (C) (lower part) regions. Except for some values in the region (B) in beginning of the Table III, our results are in good agreement with experimental data, concerning both the $B(E2)$ values and the HF's. The value $R_1 = 0$ would correspond to an isoscalar symmetry for equal strengths.

Because $R_2 = -0.75$, the neutron strength dominates over the proton one ($V_\nu = 7V_\pi$), but at the same time it is comparable with the proton-neutron strength, $V_{\pi\nu} \approx 0.57V_\nu$. We stress that these strengths were obtained as the best fit result for $B(E2)$ values. Consequently, the neutron-proton asymmetry is at least partially explained by the use of a vanishing neutron charge in the transition operator. On the other hand, the HF's, obtained by using an independent approach, seem to confirm the validity of this result. Still, because of the relative small number of experimental data on α-decay intensities to excited states, a further investigation is necessary.

The phase transition in region (B) was reproduced by using different values of the ratio parameter R_1. Thus, the first two large HF's can be reproduced by using $R_1 = 0.5$, with the same R_2. For the moment, we do not have experimental data concerning $B(E2)$ values for these nuclei, and we can only point out this interesting feature.

We should also point out that several nuclei as ^{216,218}Po, ^{218,220}Rn, ^{218}Ra have important octupole deformations [34]. Concerning Po isotopes, our systematics indeed predicts HF's that are three times, larger, but for the remaining nuclei they are within the experimental errors. At the same time, let us mention that the excitation energies for Rn and Ra isotopes are two times less than in the case of Po isotopes. According to Eq. (3.3), the HF depends exponentially upon the excitation energy. Thus, the influence of octupole vibrations becomes indeed stronger in the former case.

Finally, we should point out that the spectroscopic factors for transitions connecting ground states, computed by using Eq. (2.15), have similar values for the decays below Pb, namely, $S_\alpha^{(0)} \approx 5 \times 10^{-3}$. For decays above Pb, we obtained $S_\alpha^{(0)} \approx 10^{-3}$. This gives the order of magnitude of the α-decay preformation probability, which agrees with the estimate of Ref. [37].

Thus we show once again that α-decay fine structure involving the first 2^+ state is a more sensitive tool for probing

the residual interaction than is the electromagnetic transition deexiting the first 2^+ state.

IV. CONCLUSIONS

In this article we presented a systematics of the α-decay HF and $B(E2)$ values of the first excited 2^+ states in even-even nuclei. We computed the α-decay HF within the spherical QRPA formalism. The single-particle spectrum is given by a diagonalization procedure of the Woods-Saxon mean field with the universal parametrization. We considered as a residual force a realistic two-body interaction, obtained from the G-matrix elements of the Bonn interaction. The only free parameters will the ratio of the isovector to the isoscalar strength R_1 and the proton-neutron asymmetry R_2.

We performed a systematic analysis of the HF and $B(E2)$ values versus these ratios and the energy E_{2^+} of the first collective state. This formalism was able to explain the main trends seen in the systematics of experimental data, namely, the universal decrease of the $B(E2)$ value and the increase of the HF with increasing energy E_{2^+} along any neutron chain. Moreover, the specific character of each isotope chain, concerning the slope of the HF versus E_{2^+}, could be explained by concrete nuclear structure details. We proposed an empirical linear dependence between the logarithm of the hindrance factor and the lowest energy E_{2^+}. This dependence was confirmed by our QRPA calculations.

We found out that most of the existing experimental data concerning the $B(E2)$ value and HF could be reproduced by using a single set of parameters, namely $R_1 = 0$, $R_2 = -0.75$, except for very neutron-deficient nuclei, where $R_1 = 0.5$.

ACKNOWLEDGMENTS

This work has been supported by the Academy of Finland under the Finnish Centre of Excellence Programme 2000–2005 (Project No. 44875, Nuclear and Condensed Matter Programme at JYFL). One of us (D.S.D.) is thankful for the hospitality extended to him by the Department of Physics of the University of Jyväskylä, where part of this work was performed. Discussions with R. Julin and M. Leino (Jyväskylä) are gratefully acknowledged.

[1] G. Gamow, Z. Phys. **51**, 204 (1928).
[2] R. G. Thomas, Prog. Theor. Phys. **12**, 253 (1954); A. M. Lane and R. G. Thomas, Rev. Mod. Phys. **30**, 257 (1958).
[3] H. J. Mang, Annu. Rev. Nucl. Sci. **14**, 1 (1964).
[4] J. K. Poggenburg, H. J. Mang, and J. O. Rasmussen, Phys. Rev. **181**, 1697 (1969).
[5] D. S. Delion, A. Sandulescu, and W. Greiner, Phys. Rev. C **69**, 044318 (2004).
[6] J. O. Rasmussen, Phys. Rev. **113**, 1593 (1959).
[7] J. O. Rasmussen and B. Segal, Phys. Rev. **103**, 1298 (1956).
[8] H. M. A. Radi, A. A. Shihab-Eldin, J. O. Rasmussen, and Luiz F. Oliveira, Phys. Rev. Lett. **41**, 1444 (1978).
[9] P. O. Fröman, Kgl. Dan. Vidensk. Selsk. Mat.-Fys. **1**, 3 (1957).
[10] A. Sandulescu and O. Dumitrescu, Phys. Lett. **19**, 404 (1965).
[11] A. Sandulescu and O. Dumitrescu, Phys. Lett. **B24**, 212 (1967).
[12] M. I. Cristu, O. Dumitrescu, N. I. Pyatov, and A. Sandulescu, Nucl. Phys. **A130**, 31 (1969).
[13] D. S. Delion, A. Florescu, M. Huyse, J. Wauters, and P. Van Duppen (ISOLDE Collaboration), Phys. Rev. Lett. **74**, 3939 (1995); Phys. Rev. C **54**, 1169 (1996).
[14] J. Wauters, P. Dendooven, P. Decrock, M. Huyse, R. Kirchner, O. Klepper, G. Reusen, E. Roeckl, and P. Van Duppen, Z. Phys. A **342**, 277 (1992).
[15] J. Wauters, P. Dendooven, M. Huyse, G. Reusen, P. Lievens, P. Van Duppen (ISOLDE Collaboration), Z. Phys. A **344**, 29 (1992).
[16] J. Wauters, P. Dendooven, M. Huyse, G. Reusen, P. Van Duppen, R. Kirchner, O. Klepper, and E. Roeckl, Z. Phys. A **345**, 21 (1993).
[17] J. Wauters, P. Dendooven, M. Huyse, G. Reusen, P. Van Duppen, and P. Lievens (ISOLDE Collaboration), Phys. Rev. C **47**, 1447 (1993).
[18] J. Wauters, N. Bijnens, H. Folger, M. Huyse, H. Y. Hwang, R. Kirchner, and J. von Schwarzenberg, Phys. Rev. C **50**, 2768 (1994).
[19] J. Wauters *et al.*, Phys. Rev. Lett. **72**, 1329 (1994).
[20] N. Bijnens *et al.*, Phys. Rev. Lett. **75**, 4571 (1995).
[21] R. G. Allatt *et al.*, Phys. Lett. **B437**, 29 (1998).
[22] C. F. Liang, R. K. Sheline, P. Paris, M. Hussonnois, J. F. Ledu, and D. B. Isabelle, Phys. Rev. C **49**, 2230 (1994).
[23] C. N. Davids and H. Esbensen, Phys. Rev. C **64**, 034317 (2001).
[24] K. Hagino, Phys. Rev. C **64**, 041304(R) (2001).
[25] D. S. Delion and R. J. Liotta, Phys. Rev. C **56**, 1782 (1997).
[26] D. S. Delion and J. Suhonen, Phys. Rev. C **64**, 064302 (2001).
[27] D. S. Delion, A. Insolia, and R. J. Liotta, Phys. Rev. C **46**, 1346 (1992).
[28] T. Fliessbach and S. Okabe, Z. Phys. A **320**, 289 (1985).
[29] D. S. Delion, A. Insolia, and R. J. Liotta, Phys. Rev. C **54**, 292 (1996).
[30] D. S. Delion and J. Suhonen, Phys. Rev. C **61**, 024304 (2000).
[31] S. Raman, C. W. Nestor, Jr., and P. Tikkanen, At. Data Nucl. Data Tables **78**, 1 (2001).
[32] S. Raman, C. W. Nestor, S. Kahane, and K. H. Bhatt, Phys. Rev. C **43**, 556 (1991).
[33] Y. A. Akovali, Nucl. Data Sheets **84**, 1 (1998).
[34] P. Möller, J. R. Nix, W. D. Myers, and W. J. Swiatecki, At. Data Nucl. Data Tables **59**, 185 (1995).
[35] J. Dudek, Z. Szymanski, and T. Werner, Phys. Rev. C **23**, 920 (1981).
[36] K. Holinde, Phys. Rep. **68**, 121 (1981).
[37] R. Blendowske, T. Fliessbach, and H. Walliser, Nucl. Phys. **A464**, 75 (1987).